

See discussions, stats, and author profiles for this publication at: <https://www.researchgate.net/publication/234880150>

Femtosecond mid-infrared spectroscopy of aqueous solvation shells

ARTICLE *in* THE JOURNAL OF CHEMICAL PHYSICS · NOVEMBER 2001

Impact Factor: 2.95 · DOI: 10.1063/1.1412249

CITATIONS

79

READS

29

2 AUTHORS, INCLUDING:



Huib J Bakker

FOM Institute AMOLF

241 PUBLICATIONS 8,702 CITATIONS

SEE PROFILE

Femtosecond mid-infrared spectroscopy of aqueous solvation shells

M. F. Kropman and H. J. Bakker

FOM Institute AMOLF, Kruislaan 407, 1098 SJ Amsterdam, The Netherlands

(Received 18 June 2001; accepted 27 August 2001)

We use femtosecond two-color mid-infrared spectroscopy to study the dynamics of aqueous solutions of salts in HDO:D₂O. We find that the lifetime of the O–H stretch vibration of HDO molecules in the solvation shell of the halogenic anions Cl[−], Br[−], and I[−] is much longer than the lifetime of the O–H stretch vibration of the HDO molecule in bulk D₂O solution. This difference in lifetime allows for a clear separation of the response of the solvation shell from that of the bulk liquid. A detailed investigation of the spectral dynamics of the solvating HDO molecules reveals that the hydrogen-bond dynamics of these molecules are much slower than the hydrogen-bond dynamics of bulk liquid water. © 2001 American Institute of Physics. [DOI: 10.1063/1.1412249]

I. INTRODUCTION

The dynamics of chemical reactions in aqueous media are strongly dependent on the interactions between the reacting molecules and the solvating water molecules. Unfortunately, the experimental study of aqueous solvation interactions is not without problems, because it requires the response of the solvating water molecules to be distinguished from that of the other (bulk) water molecules. In general, this distinction cannot be made with conventional linear spectroscopic techniques. As a result, aqueous solvation forms one of the less understood interactions in chemical physics.

The contribution of bulk water to the response of an aqueous solution can be eliminated by studying small clusters of an ion surrounded by a few water molecules in the gas phase.^{1–4} In these studies evidence was found that halogenic anions like F[−], Cl[−], Br[−], and I[−] are solvated by water via directional hydrogen-bond interactions. It was also observed and calculated that the structure of these clusters strongly depends on the number of water ligands.^{5–7} For small numbers of ligands, the water molecules tend to cluster at one side of the ion (surface structures).^{5,6} Only at large numbers of liquid water molecules, the ion is engaged by the water molecules (internal structures).

Bulk aqueous solutions of salts have been investigated with infrared⁸ and continuous wave (cw) Raman spectroscopy.^{9–11} For most anions, the water molecules are bound by directional O–H···Y[−] hydrogen bonds. For Y[−] = Cl[−], Br[−], I[−], the O–H···Y[−] hydrogen bond is observed to be weaker than the O–H···O hydrogen bond between two water molecules, and is observed to become weaker within the halogenic series. The same trend is observed in vibrational predissociation experiments¹² and molecular dynamics (MD) simulations¹³ on small clusters. The information obtained from infrared and Raman studies on the structure of aqueous solvation shells is quite limited, since the observed changes in the shape of the Raman spectrum both result from solvation interactions between water and dissolved ions and from changes in the bulk water structure. The structure of the solvation shells of ions in bulk aqueous solutions has also been investigated with nuclear magnetic resonance (NMR)

(Ref. 14) and molecular dynamics simulations.^{15–19} From these studies information was obtained on the number of water molecules in the first solvation shell of the ion and on the distance between these molecules and the ion.

Unfortunately, techniques like NMR, infrared absorption, and Raman scattering cannot be used to study the dynamics of aqueous solvation shells, because the time scales involved in these techniques are much longer than the time scale of the solvation dynamics. Hence, the information on these dynamics is mainly theoretical in nature and originates from molecular dynamics simulations.^{20–24} In these studies strongly different time constants for the exchange of water molecules between the solvation shell and the bulk were reported, ranging from one picosecond up to hundreds of picoseconds.^{22,23}

An elegant method to get experimental information on the dynamics of aqueous solvation shells that circumvents the problem of the strong inhomogeneity of an aqueous system, is by exciting and detecting a probe molecule dissolved in water.²⁵ In this type of experiment, information on the dynamics of the solvating water molecules is inferred from the time-dependent response of the probe molecule. For instance, it was observed that the fluorescence of a dye molecule dissolved in water shows a very rapid red-shift with a time constant smaller than 50 fs, which indicates that solvating water molecules can show a very rapid rearrangement. A disadvantage of this technique is that it probes the dynamics and structure of the solvating water molecules rather indirectly.

Recently, it has become possible to study the structure and dynamics of water molecules directly with a nonlinear spectroscopic technique that probes the response of the O–H stretch vibrations of the water molecule.^{26–33} In this technique the O–H stretch vibration of the water molecules is excited with an intense ultrashort mid-infrared pulse and the dynamics of this excitation are probed using a second weak ultrashort mid-infrared or visible pulse. With this technique, new information on the structure and dynamics of neat liquid water was obtained. For instance, it was found that the reorientational motion of water shows a bimodal distribution that

is strongly correlated to the strength of the hydrogen-bond interactions between the water molecules.²⁷

Up to now, most ultrafast mid-infrared spectroscopic studies on aqueous systems have been performed on neat liquid water, e.g., pure liquid H₂O and dilute solutions of HDO in D₂O,^{26–33} and the electron solvated in water.³⁴ However, recently the technique was used to investigate the dynamics of aqueous solvation interactions.³⁵ Here we present a more detailed femtosecond mid-infrared spectroscopic study of the dynamics of water molecules in bulk aqueous solutions by studying solutions of different salts, concentrations, and temperatures.

II. EXPERIMENT

The experiment is a two-color pump–probe experiment using independently tunable femtosecond mid-infrared laser pulses. The pulses are generated via parametric frequency-conversion processes that are pumped with the pulses delivered by a Ti:sapphire regenerative amplifier. These pulses have a central wavelength of 800 nm, an energy per pulse of 3 mJ and a pulse duration of approximately 120 fs. The repetition rate of the system is 1 kHz. In a first multipass parametric generation process in a BBO crystal of 4 mm length, part of the pulse at 800 nm is converted into signal and idler pulses at wavelengths of approximately 1250 nm and 2200 nm, respectively. The pulse at 2200 nm is frequency doubled in a second BBO crystal of 2 mm length to generate a pulse at 1100 nm. This pulse is used as a seed pulse in a parametric amplification process in a 5 mm KTP crystal that is pumped by another part of the 800 nm pulse. This process results in the amplification of the pulse at 1100 nm and the generation of a pulse with a wavelength of approximately 3000 nm that is used in the experiment. We use two chains of parametric generation and amplification processes in order to generate pump and probe pulses that are independently tunable. The wavelength of these pulses can easily be varied between 2.7 and 4 μ m by rotating the BBO and KTP crystals. The pulses have a typical energy of 20/2 μ J (pump/probe) and a duration of approximately 200 fs.³¹ The spectral bandwidths of the pump and probe pulses are 80 and 60 cm^{-1} , respectively.

We performed femtosecond mid-infrared pump–probe experiments on the O–H stretch vibration of HDO molecules in an aqueous solution consisting of a low concentration of HDO (0.1 M) in D₂O and different concentrations (1 M, 2 M, 3 M, 6 M) of KF, NaCl, NaBr, NaI, and MgCl₂. The intense mid-infrared pump pulse excites a significant fraction of the HDO molecules to the first excited state ($\nu = 1$) of the O–H stretch vibration. The energy relaxation and spectral dynamics of this excitation are probed with the weak, independently tunable probe pulse. The polarization of the probe pulse is at the magic angle (54.7°) with respect to the polarization of the pumping pulse in order to avoid the measurements to be affected by reorientation of the HDO molecules. In the experiments, both the pump and probe frequencies are tuned through the absorption band of the O–H stretching mode of the HDO molecules.

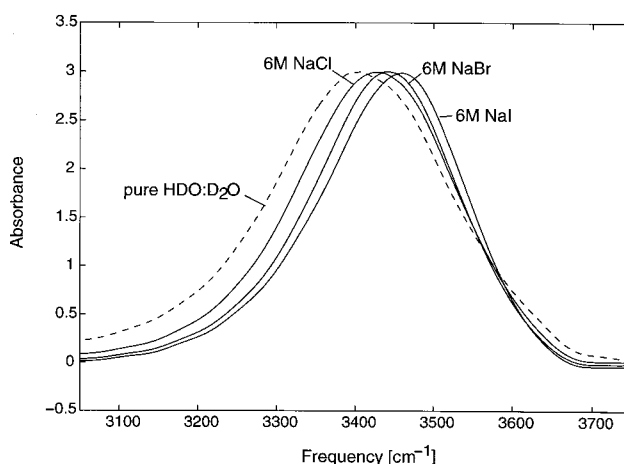


FIG. 1. Absorption spectra of a solution of 0.5 M HDO in D₂O and of solutions of 6 M NaCl, NaBr and NaI in the HDO:D₂O solution.

III. RESULTS

In Fig. 1, the absorption spectrum of the O–H stretch vibration of HDO is shown for solutions 6 M of NaCl, NaBr or NaI in HDO:D₂O. Within the halogenic series Cl[−], Br[−], and I[−], the absorption spectrum of the O–H stretch vibration is observed to shift to higher frequencies.

In Fig. 2, delay scans are presented measured at a pump frequency of 3400 cm^{-1} and six different probe frequencies for a solution of 6 M NaI in HDO:D₂O. At frequencies $\geq 3350 \text{ cm}^{-1}$, a bleaching [$\ln(T/T_0) > 0$, with T the transmission of the probe and T_0 the transmission of the probe in absence of the pump] of the $\nu = 0 \rightarrow 1$ transition is observed. At frequencies $\leq 3300 \text{ cm}^{-1}$, an induced absorption [$\ln(T/T_0) < 0$] is observed, which can be assigned to the induced $\nu = 1 \rightarrow 2$ transition. With increasing delay, the bleaching and induced absorption decay due to the energy relaxation of the $\nu = 1$ state of the O–H stretch vibration of the excited HDO molecules.

In Figs. 3–5, transients measured for three different salts

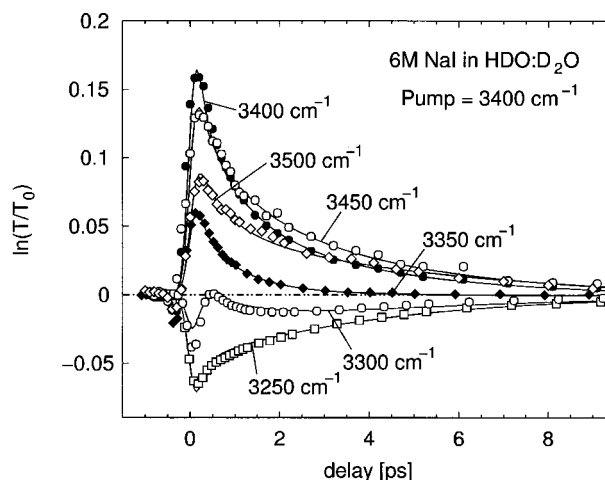


FIG. 2. Pump–probe transients measured for an aqueous solution of 6 M NaI in HDO:D₂O. The transients are measured at six different probe frequencies and a pump frequency of 3400 cm^{-1} . The solid curves are calculated with the Brownian oscillator model described in the text.

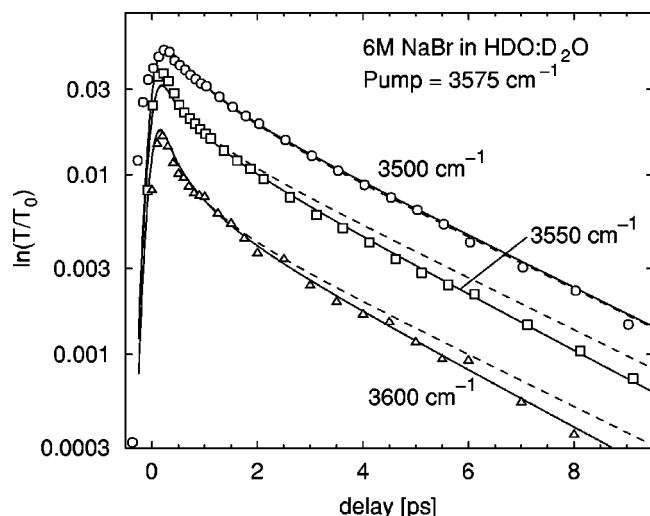


FIG. 3. Pump-probe transients measured for an aqueous solution of 6 M NaBr in HDO:D₂O. The transients are scaled with respect to each other and are plotted on a logarithmic scale to clarify the presence of two absorption components and the difference in time constant. The solid curves are calculated with the Brownian oscillator model of the slow component using a τ_c of the modulation of the O-H \cdots Br⁻ hydrogen bond of 25 ps. The dashed curves are calculated with the same model using $\tau_c = \infty$.

are presented. The transients are shown on a vertical logarithmic scale to illustrate that at all frequencies the decay is nonexponential and consists of a rapid decay followed by a much slower decay. The curves are scaled with respect to each other for clarity. The amplitude of the signals depends on both the pump and probe frequencies. For a solution of NaCl, the largest amplitude is observed for pump and probe frequencies of approximately 3450 cm⁻¹, whereas for solutions of NaBr and NaI, the largest amplitude is observed for pump and probe frequencies of approximately 3500 cm⁻¹. All transients can be described as a sum of two exponentials, one with a time constant of 800 fs and one with a longer time constant that depends on salt and probe frequency. The am-

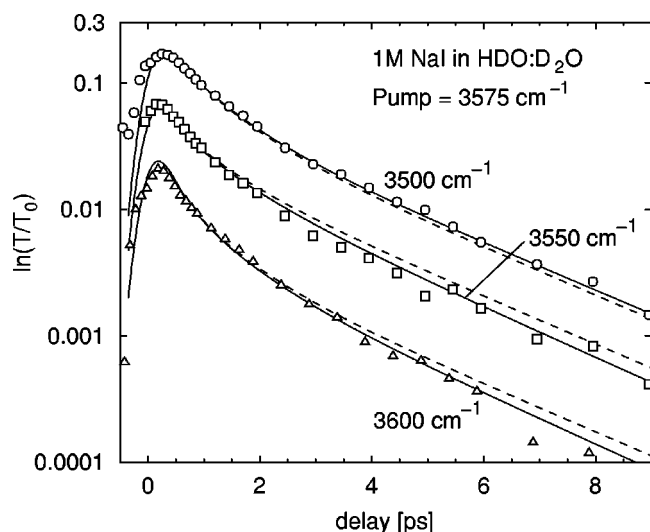


FIG. 4. As Fig. 3, but for a solution of 1 M NaI in HDO:D₂O. The solid curves are calculated using a τ_c of the modulation of the O-H \cdots I⁻ hydrogen bond of 18 ps. The dashed curves are calculated with $\tau_c = \infty$.

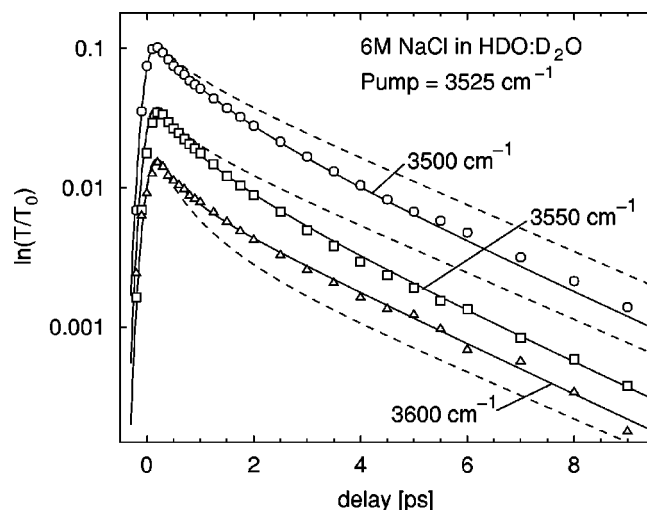


FIG. 5. As Fig. 3, but for a solution of 6 M NaCl in HDO:D₂O. The solid curves are calculated using a τ_c of the modulation of the O-H \cdots Cl⁻ hydrogen bond of 12 ps. The dashed curves are calculated with $\tau_c = \infty$.

plitude of the slow component depends linearly on the concentration of dissolved salt. Interestingly, changing the nature of the cation has no effect on the experimental observations: Solutions of NaCl and MgCl₂ give exactly the same results, as long as the concentration of Cl⁻ ions is the same. In contrast, the time constant does strongly depend on the anion, and increases within the halogenic series F⁻, Cl⁻, Br⁻, and I⁻.

The time constant of the slow component shows a small but significant dependence on the probe frequency. To illustrate this more clearly, Figs. 3–5 contain calculated dashed curves that run parallel at large delay times (>3 ps). The time constant of the slow component is observed to increase with increasing frequency difference between pump and probe. If the pump is at 3575 cm⁻¹ (Figs. 3 and 4), the fastest decay is observed at 3600 cm⁻¹ and the slowest decay at 3500 cm⁻¹. If the pump is at 3525 cm⁻¹ (Fig. 5), the fastest decay is observed at 3500 cm⁻¹ and the slowest decay at 3600 cm⁻¹. These observations show that the decay time constant of the slow component is affected by a slow spectral diffusion process with a time constant of approximately 10 ps. Due to this spectral diffusion process, excited molecules (spectrally) diffuse away from the excitation frequency, which leads to a faster decay at probe frequencies close to the pump frequency and a slower decay at probe frequencies that significantly differ from the pump frequency.

In Fig. 6, transients are presented that are measured for a solution of 3 M NaCl in HDO:D₂O at three different temperatures. At all three temperatures, the transient measured at 3600 cm⁻¹ is observed to decay somewhat faster than the transient at 3450 cm⁻¹, as a result of the above mentioned spectral diffusion. An interesting observation is that the difference in decay rate of the two transients decreases with temperature: At a temperature of 85 °C the two transients show a more similar decay than at room temperature. This observation indicates that the spectral diffusion becomes slower when the temperature increases.

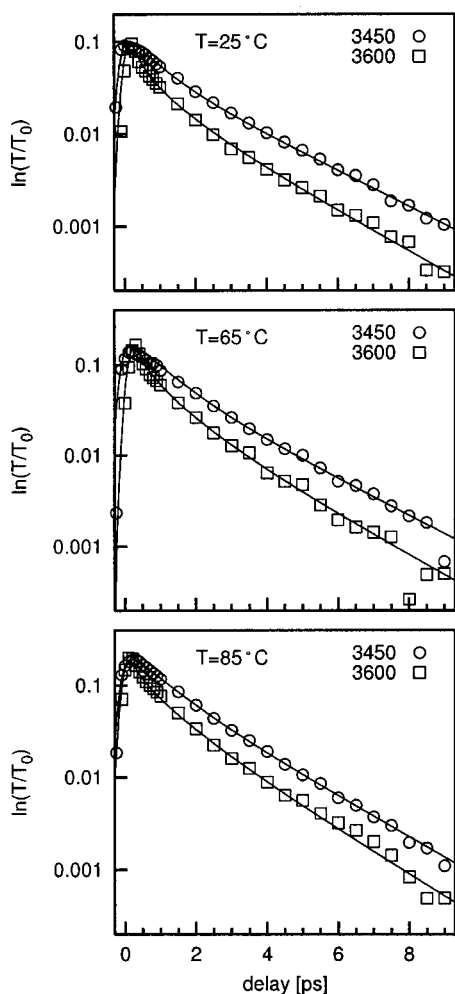


FIG. 6. Pump-probe transients measured for a solution of 3 M NaCl in HDO:D₂O at three different temperatures. The difference in final decay time of the slow component decreases with increasing temperature which means that the value of τ_c of the modulation of the O-H \cdots Cl⁻ hydrogen bond increases. The solid curves are calculated using $\tau_c = 14$ ps (25 °C), $\tau_c = 24$ ps (65 °C), and $\tau_c = 30$ ps (85 °C).

IV. INTERPRETATION

A. Vibrational lifetimes of HDO in aqueous solvation shells

In an aqueous solution of a salt in HDO:D₂O, three different types of HDO molecules can be distinguished: HDO molecules in the first solvation shell of the anion, HDO molecules in the first solvation shell of the cation and HDO molecules that are only surrounded by D₂O molecules. In the following, these latter molecules will be denoted as bulk HDO molecules. The three different types of HDO molecules give rise to the fast and the slow component observed in the transient spectral data of Figs. 2–6.

The amplitude and time constant of the fast component do not depend on the concentration of dissolved salt, which suggests that this component results from bulk HDO molecules. This interpretation is supported by the observation that the fast component has a time constant of 800 fs, which is very similar to the vibrational lifetime T_1 observed for a solution of HDO in D₂O.²⁹ The observation that the amplitude and time constant of the slow component do not depend

on the nature and concentration of the cations, indicates that the fast component also contains the contribution of the HDO molecules in the first solvation shell of the cation. For these HDO molecules, the O–H groups will point away from the ion and will form O–H \cdots O hydrogen bonds with bulk D₂O molecules.^{15–17} For O–H \cdots O hydrogen-bonded systems, it has been found that the lifetime of an O–H stretch vibration strongly depends on the strength of the O–H \cdots O hydrogen-bond interaction.^{36,38} The O–H \cdots O hydrogen bonds formed by HDO molecules in the first solvation shell of the cation with bulk D₂O molecules will be similar to the hydrogen bonds formed between bulk HDO and bulk D₂O. As a result, the O–H stretch vibration of a HDO molecule in the first solvation shell of the cation is indeed expected to have a similar vibrational lifetime T_1 as the O–H stretch vibration of a bulk HDO molecule.

From the dependence of the time constant and amplitude of the slow component on the nature and concentration of dissolved anions, and from the absence of such a dependence for the cations, it follows that the slow component results from HDO molecules that solvate the anion. The decay time constants of 2.6 ± 0.2 ps, 3.0 ± 0.2 ps, and 3.7 ± 0.3 ps observed for the slow component in solutions of Cl⁻, Br⁻, and I⁻, respectively, thus reflect the vibrational lifetime of the O–H stretch vibration of an HDO molecule in the first solvation shell of these halogenic ions.

The relatively long vibrational lifetime of the HDO molecule in the first solvation shell of the anions can be explained if the O–H \cdots Y⁻ hydrogen bond accepts (part of) the energy of the O–H stretch vibration. In a solution of HDO:D₂O, the O–H stretch vibrational energy is accepted either by a combination of the HOD bending mode³³ and the O–H \cdots O hydrogen bond, or by the hydrogen bond alone.³⁷

There are at least two ways in which the properties of the O–H \cdots Y⁻ hydrogen bond can account for the longer vibrational lifetimes for larger anions. First, the O–H stretch frequency increases (the red-shift from the gas-phase value decreases) in the series F⁻, Cl⁻, Br⁻, I⁻ (see Fig. 1 and Refs. 8, 12), which indicates a decreasing hydrogen-bond strength.³⁸ The weaker hydrogen-bond interaction in turn leads to a decrease of the anharmonic interaction terms between the O–H stretch vibration and the hydrogen-bond mode.³⁸

Second, the reduced mass of the O–H \cdots Y⁻ hydrogen-bond stretch vibration, which determines the energy spacing of the levels of this mode increases within the halogenic series F⁻, Cl⁻, Br⁻, I⁻. As a result, the level spacing of the hydrogen-bond vibration decreases. For I⁻, therefore, a higher level of the hydrogen-bond vibration must be excited than for F⁻, in order to dissipate the same amount of energy. Hence, the anharmonic interaction term responsible for the energy relaxation of O–H \cdots I⁻ will be of higher order in the hydrogen-bond coordinate than the anharmonic interaction term responsible for the relaxation of O–H \cdots Cl⁻. In general, the magnitude of the anharmonic interaction decreases with increasing order in the vibrational coordinates.^{38,39} At this moment, it is not clear which of the two above-mentioned effects, anharmonic interaction strength or re-

duced mass of the hydrogen-bond vibration, is most important in slowing down the relaxation in the $\text{O}-\text{H}\cdots\text{Y}^-$ series.

For a solution of KF in $\text{HDO}:\text{D}_2\text{O}$, we did not observe a slow component, which indicates that the vibrational lifetime of a HDO molecule solvating this anion is comparable to that of HDO dissolved in D_2O . For this solution, the absorption spectrum is slightly red-shifted with respect to the absorption spectrum of HDO dissolved in D_2O , and the reduced mass of the $\text{O}-\text{H}\cdots\text{F}^-$ hydrogen bond is similar to that of the $\text{O}-\text{H}\cdots\text{O}$ hydrogen bond. The absence of a slow component for solutions of F^- is consistent with the above explanation for the long T_1 of HDO molecules in the first solvation shell of Cl^- , Br^- , and I^- .

B. Hydrogen-bond dynamics of HDO in aqueous solvation shells

The pump- and probe-frequency dependence of the dynamics of the slow component (Figs. 2–6) shows that the response of this component is affected by a slow spectral diffusion process with a time constant of approximately 10 ps. This spectral diffusion directly reflects the (stochastic) modulation of the hydrogen-bond length because the transition frequency of the $\text{O}-\text{H}$ stretch vibration and the length of the hydrogen bond are strongly correlated for directional hydrogen bonds.^{40–42}

For a bulk solution of HDO in D_2O , the spectral diffusion of the $\text{O}-\text{H}$ stretch absorption band was observed to be very fast, having a correlation time constant τ_c of approximately 500 fs.^{30,31} As a result, the excited spectrum (spectral hole) of the $\text{O}-\text{H}$ stretch vibration of HDO dissolved in D_2O was observed to acquire the shape of the linear absorption spectrum within a few picoseconds.³⁰ The much longer time scale of the spectral diffusion of the slow absorption component observed for the aqueous salt solutions indicates that the stochastic modulation of the $\text{O}-\text{H}\cdots\text{Y}^-$ hydrogen-bond length is significantly slower than the stochastic modulation of the $\text{O}-\text{H}\cdots\text{O}$ hydrogen-bond length in bulk liquid water.

In order to determine the precise value of the correlation time constant τ_c of the stochastic modulation of the $\text{O}-\text{H}\cdots\text{Y}^-$ hydrogen bond, we modeled the data of Figs. 2–6 with the Brownian oscillator model.⁴³ Recently it was shown that this model works well in describing the spectral dynamics of the $\text{O}-\text{H}$ stretching mode of HDO dissolved in D_2O induced by the interactions with the $\text{O}-\text{H}\cdots\text{O}$ hydrogen bond.³¹ The determination of τ_c of the $\text{O}-\text{H}\cdots\text{Y}^-$ hydrogen bond is greatly facilitated by the large difference in vibrational lifetime between the $\text{O}-\text{H}\cdots\text{O}$ and the $\text{O}-\text{H}\cdots\text{Y}^-$ component ($\text{Y}^- = \text{Cl}^-$, Br^- , I^-). Due to this difference in lifetime, a transient spectrum measured after a few picoseconds only contains contributions from the molecules in the first solvation shell of the anion.

The Brownian oscillator model assumes harmonic-potential energy functions for the low-frequency mode (hydrogen bond) that are displaced with respect to each other in the ground and excited state of the $\text{O}-\text{H}$ stretch oscillator. In case the hydrogen bond is a strongly overdamped mode, this results in a Gaussian absorption spectrum for the $\text{O}-\text{H}$ stretch vibration, in quite good agreement with the experimental observations. Within the Brownian oscillator model,

the spectral dynamics of the transition of the $\text{O}-\text{H}$ stretch vibrational transition is described with two parameters: the correlation time constant τ_c , representing the time scale at which the hydrogen-bond length is stochastically modulated, and the width Δ of the Gaussian absorption line shape $e^{-\omega^2/2\Delta^2}$ of the $\text{O}-\text{H}$ stretch vibration. This width increases with increasing displacement of the harmonic-potential energy functions. An explicit expression for the pump–probe signal S_{pp} as a function of delay τ and pump and probe frequency can be found in the literature,⁴³

$$S_{\text{pp}}(\omega_1, \omega_2, \tau) = \frac{2\pi e^{-\tau/T_1}}{\sqrt{(\Delta^2 + \delta_1^2)\alpha^2(\tau)}} e^{(-\omega_1 - \omega_{eg})^2/2(\Delta^2 + \delta_1^2)} \times \{e^{-[\omega_2 - \omega_g(\tau)]^2/2\alpha^2(\tau)} + e^{-[\omega_2 - \omega_e(\tau)]^2/2\alpha^2(\tau)}\}, \quad (1)$$

with

$$\omega_g(\tau) = \omega_{eg} + e^{-\tau/\tau_c}(\omega_0 - \omega_{eg}), \quad (2)$$

$$\omega_e(\tau) = \omega_{eg} - 2\lambda + e^{-\tau/\tau_c}(\omega_0 - \omega_{eg} + 2\lambda), \quad (3)$$

$$\lambda = \hbar\Delta^2/2k_B T, \quad (4)$$

$$\omega_0 = \omega_1 \frac{\Delta^2}{\Delta^2 + \delta_1^2} + \omega_{eg} \frac{\delta_1^2}{\Delta^2 + \delta_1^2}, \quad (5)$$

$$\alpha^2(\tau) = \Delta^2 \left[1 - \frac{\Delta^2}{\Delta^2 + \delta_1^2} e^{-\tau/\tau_c} \right] + \delta_2^2, \quad (6)$$

where ω_1 , δ_1 and ω_2 , δ_2 are the center frequencies and the spectral widths of pump and probe, respectively. The frequency ω_{eg} is the maximum of the linear absorption spectrum and T_1 is the vibrational lifetime. The parameter λ represents the Stokes shift ($=2\lambda$) that results from the fact that the position of the minimum of the hydrogen-bond potential of the excited state of the $\text{O}-\text{H}$ stretch vibration differs from that of the ground state. Hence, excitation of the $\text{O}-\text{H}$ stretch vibration results in a shift of the hydrogen-bond length to a new equilibrium position and an associated red-shift of 2λ of the stimulated emission out of the $v=1$ potential to the $v=0$ potential. For harmonic potentials, the Stokes shift is directly related to the width Δ of the absorption band. λ itself does not depend on temperature, since it is only determined by the shape and displacement of the harmonic potentials. Nevertheless, in expression (4) the temperature T enters, because the width Δ of the absorption band depends on the thermal occupation of the ground-state potential in such a manner that λ is temperature independent. The two terms between the braces in Eq. (1) correspond to the bleaching (depletion of the $v=0$) and to the stimulated emission $v=1 \rightarrow 0$ contribution to the transmission change $\ln(T/T_0)$.

For all transients, we find an excellent fit using two Brownian oscillators that represent the $\text{O}-\text{H}\cdots\text{O}$ and $\text{O}-\text{H}\cdots\text{Y}^-$ components. In Table I, the central frequency ω_{eg} , the spectral width $\Delta\omega$ (full width at half maximum, $\Delta\omega = \sqrt{8 \ln 2} \Delta$), the vibrational lifetime T_1 , and the correla-

TABLE I. The central frequency ω_0 , width $\Delta\omega$, vibrational lifetime T_1 , and spectral diffusion time τ_c of the O–H stretch vibration of different hydrogen-bonded O–H groups, obtained by fitting the data using a two-component Brownian oscillator model, described in the text. The values are obtained for 6 M solutions of NaCl, NaBr, and NaI. For all solutions, the same set of values for the O–H \cdots O component was used.

	ω_0	$\Delta\omega$	T_1	τ_c
O–H \cdots O	$3420 \pm 10 \text{ cm}^{-1}$	$280 \pm 20 \text{ cm}^{-1}$	$0.8 \pm 0.1 \text{ ps}$	$0.5 \pm 0.2 \text{ ps}$
O–H \cdots Cl $^-$	$3440 \pm 15 \text{ cm}^{-1}$	$160 \pm 15 \text{ cm}^{-1}$	$2.6 \pm 0.2 \text{ ps}$	$12 \pm 3 \text{ ps}$
O–H \cdots Br $^-$	$3470 \pm 15 \text{ cm}^{-1}$	$130 \pm 15 \text{ cm}^{-1}$	$3.0 \pm 0.2 \text{ ps}$	$25 \pm 5 \text{ ps}$
O–H \cdots I $^-$	$3490 \pm 15 \text{ cm}^{-1}$	$105 \pm 15 \text{ cm}^{-1}$	$3.7 \pm 0.3 \text{ ps}$	$18 \pm 5 \text{ ps}$

tion time τ_c that result from these fits are presented for the different absorption components. The results are shown in Table I.

For all solutions, we find the same set of parameters for the O–H \cdots O component. The parameters of this oscillator are quite similar to those of HDO dissolved in D₂O. Only the width of the absorption band appears to be slightly larger, which can be explained from the contribution of HDO molecules solvating the cations. The results of the calculations are shown in Figs. 2–6 by the solid curves. The measurements are sensitive to the value of the correlation time constant τ_c . We find $\tau_c = 12 \pm 3$ for Cl $^-$, $\tau_c = 25 \pm 5$ for Br $^-$, and $\tau_c = 18 \pm 5$ for I $^-$. For comparison, in Figs. 3–5 also results obtained with $\tau_c = \infty$ are shown (dashed curves). The calculated dashed curves run parallel at large delays, because for $\tau_c = \infty$ the transients are no longer affected by spectral diffusion. This behavior is in clear contrast to the experimental observations and the calculated solid curves.

The frequencies of the O–H \cdots Cl $^-$, O–H \cdots Br $^-$, and O–H \cdots I $^-$ absorption components are in quite good agreement with the results from a study in which a double-difference spectroscopic technique was used to obtain the change in O–D stretch frequency due to salt addition.⁸ After multiplying by 1.36 to convert O–D into O–H stretch frequencies,⁴⁴ the central absorption frequencies they found are 3441 cm^{-1} (O–H \cdots Cl $^-$), 3476 cm^{-1} (O–H \cdots Br $^-$), and 3495 cm^{-1} (O–H \cdots I $^-$).

The central frequency of the absorption band of the O–H \cdots Y $^-$ component increases in the halogenic series Cl $^-$, Br $^-$, and I $^-$, whereas the width of the absorption band decreases within this series. Both trends reflect the decrease of the strength of the hydrogen-bond interaction between the solvating HDO molecule and the anion in the halogenic series. The relation between the O–H stretch vibrational frequency and the length of the O–H \cdots X has been measured for many hydrogen-bond acceptors X including the halogenic anions.^{41,42} This relation can be used to determine the distribution of O–H \cdots Y $^-$ hydrogen-bond lengths from the width of the O–H \cdots Y $^-$ absorption components. For the O–H \cdots Cl $^-$, O–H \cdots Br $^-$, and O–H \cdots I $^-$ hydrogen-bonds, we obtain widths of the length distribution of $0.20(0.05) \times 10^{-10} \text{ m}$, $0.21(0.05) \times 10^{-10} \text{ m}$, and $0.12(0.04) \times 10^{-10} \text{ m}$, respectively. These widths are relatively small compared to the width of the O–H \cdots O absorption band of HDO:D₂O of $0.36(0.02) \times 10^{-10} \text{ m}$. It should be noted that, because of homogeneous broadening, the widths of the obtained distri-

butions form upper limits; the true widths may be even narrower. The narrow width and long τ_c of the O–H \cdots Y $^-$ absorption component imply that the water molecules that directly bind to the Y $^-$ halogenic anion form a relatively stable and well-defined structure. It should be noted that the solvation shells of F $^-$ and of the cations likely show similar dynamics as the solvation shells of Cl $^-$, Br $^-$ and I $^-$, but unfortunately these dynamics could not be measured because the O–H stretch vibrational lifetime of the water molecules in these solvation shells is comparable to that of bulk HDO:D₂O.

The value of τ_c is observed to be somewhat longer for the solvation shells of Br $^-$ and I $^-$ than for the solvation shell of Cl $^-$ and τ_c is observed to increase with temperature from $12 \pm 3 \text{ ps}$ at 25 °C, to $24 \pm 5 \text{ ps}$ at 65 °C, to $30 \pm 6 \text{ ps}$ at 85 °C (Fig. 6). These observations can be well explained within the framework of the Brownian oscillator model. Following this model, the time constant τ_c is related to the frequency ω_{HB} of the hydrogen-bond stretch vibration via $\tau_c = \gamma/\omega_{\text{HB}}^2$,⁴⁵ with γ the damping of the hydrogen-bond stretch vibration. The dependence of τ_c on ω_{HB} can be understood from the fact that tight bonds (high ω_{HB}) show faster dynamics than weak bonds (low ω_{HB}), leading to a faster decay of $\langle R_{\text{HB}}(\tau)R_{\text{HB}}(0) \rangle \propto e^{-\tau/\tau_c}$.⁴⁶ The scaling of τ_c with the damping parameter γ reflects the fact that the motion in the hydrogen-bond coordinate R_{HB} will slow down when γ increases. Exchanging Cl $^-$ for Br $^-$ or I $^-$ leads to a decrease of ω_{HB} ,¹² because the hydrogen bond becomes weaker and because the reduced mass of the hydrogen-bond vibration increases. An increase in temperature also leads to a decrease of ω_{HB} , because the hydrogen-bond interaction decreases with temperature. The latter effect expresses itself in a small increase in central frequency and a decrease of the width of the O–H \cdots Y $^-$ absorption component with temperature. Hence, if the damping γ of the hydrogen-bond stretch vibration is similar for O–H \cdots Cl $^-$, O–H \cdots Br $^-$, and O–H \cdots I $^-$ hydrogen bonds, and if γ does not depend strongly on temperature, the observed increase of τ_c with temperature and going from Cl $^-$ to Br $^-$ and I $^-$, can be well explained from a decrease of the hydrogen-bond stretch frequency ω_{HB} .

The large difference between the values of τ_c of the O–H \cdots O and the O–H \cdots Y $^-$ oscillators cannot simply be explained from a difference in ω_{HB} , because the frequency ω_{HB} of the O–H \cdots Y $^-$ hydrogen-bond stretch vibration between a single water molecule and the Y $^-$ halogenic anion is only 1–2 times lower than the frequency of the O–H \cdots O hydrogen-bond stretch vibration.^{12,13} Hence, the difference in τ_c must be explained from differences in microscopic structure.

For a solvation shell, the value of the hydrogen-bond coordinate R_{HB} will be largely determined by strongly damped deformational vibrations of this shell. The frequency of these deformations will be much lower than ω_{HB} of the O–H \cdots Y $^-$ hydrogen-bond stretch vibration between a single water molecule and the Y $^-$ halogenic, because, in the liquid phase, the deformation of a relatively large solvation structure requires a reorganization of a large part of the local liquid structure. These deformational modes effectively take

the role of the Brownian oscillator in the above described model. Because the deformations are slow, the autocorrelation function $\langle R_{\text{HB}}(t)R_{\text{HB}}(0) \rangle$ will decay slowly, which implies that τ_c is large. Bulk liquid water possesses a disordered three-dimensional structure and the fluctuations that affect a local O–H···O hydrogen-bond length will involve a reorganization of only a small part of the local liquid structure. As a result, the time scale of these fluctuations will be much shorter, leading to a much faster decay of $\langle R_{\text{HB}}(t)R_{\text{HB}}(0) \rangle$.

V. CONCLUSIONS

We used two-color femtosecond mid-infrared spectroscopy to study the dynamics of the aqueous solvation shells of the halogenic anions Cl^- , Br^- , and I^- . We find that the O–H stretch vibrational lifetime of the solvating HDO molecules is 2.6 ps (Cl^-), 3.0 ps (Br^-), and 3.7 ps (I^-), which is much longer than the lifetime of 800 fs of the O–H stretch vibration of HDO dissolved in D_2O . As a result, a few picoseconds after excitation, only HDO molecules in the solvation shells of the anions remain excited, which enables a highly specific study of the spectral dynamics of these molecules.

The spectral dynamics of the solvating HDO molecules is studied by measuring transients at different probe frequencies. From this study, we find that the stochastic modulation of the length of the hydrogen bond between the water molecules and the halogenic anions has a characteristic time constant τ_c of 15–25 ps which is 20–30 times longer than the τ_c of the O–H···O hydrogen bonds of bulk liquid water. In addition, the distribution of lengths of the hydrogen bond between the water molecules and the halogenic anions is observed to be relatively narrow. Both the long τ_c and the narrow distribution of hydrogen-bond lengths indicate that the aqueous solvation shell forms a relatively long-living, well-defined structure. The value of τ_c is larger for the aqueous solvation shells of Br^- and I^- than for the solvation shell of Cl^- and is observed to increase with temperature. These observations can be well explained from the dependence of τ_c on the frequency of the hydrogen-bond vibrations between the HDO molecules and the solvated anions.

The large difference between the values of τ_c of aqueous solvation shells and bulk liquid water likely results from a strong difference in the time scale of the fluctuations that affect the length of the hydrogen bond. For an aqueous solvation shell, these fluctuations result from very slow deformations of the solvation shell that involve a reorganization of a large part of the local liquid structure. For bulk liquid water, the fluctuations that affect the hydrogen-bond length are more likely local in nature which makes them much faster.

ACKNOWLEDGMENTS

The research presented in this paper is part of the research program of the Stichting Fundamenteel Onderzoek der Materie (Foundation for Fundamental Research on Matter) and was made possible by financial support from the Nederlandse Organisatie voor Wetenschappelijk Onderzoek (Netherlands Organization for the Advancement of Research).

- ¹C. G. Bailey, J. Kim, C. E. H. Dessent, and M. A. Johnson, *Chem. Phys. Lett.* **269**, 122 (1997).
- ²J.-H. Choi, K. T. Kuwata, Y.-B. Cao, and M. Okumura, *J. Phys. Chem. A* **102**, 503 (1998).
- ³O. M. Cabarcos, C. J. Weinheimer, J. M. Lisy, and S. S. Xantheas, *J. Chem. Phys.* **110**, 5 (1999).
- ⁴P. Ayotte, C. G. Bailey, G. H. Weddle, and M. A. Johnson, *J. Phys. Chem. A* **102**, 3067 (1998).
- ⁵L. Perera and M. L. Berkowitz, *Z. Phys. D: At., Mol. Clusters* **26**, 166 (1993).
- ⁶J. E. Combariza, N. R. Kestner, and J. Jortner, *J. Chem. Phys.* **100**, 2851 (1994).
- ⁷E. D. Glendening and D. Feller, *J. Phys. Chem.* **99**, 3060 (1995).
- ⁸P.-Å. Bergström and J. Lindgren, *J. Phys. Chem.* **95**, 8575 (1991).
- ⁹G. E. Walrafen, *J. Chem. Phys.* **36**, 1035 (1962).
- ¹⁰G. E. Walrafen, *J. Chem. Phys.* **40**, 3249 (1962).
- ¹¹G. E. Walrafen, *J. Chem. Phys.* **52**, 4176 (1970).
- ¹²P. Ayotte, G. H. Weddle, J. Kim, and M. A. Johnson, *J. Am. Chem. Soc.* **120**, 12 361 (1998).
- ¹³S. S. Xantheas, *J. Phys. Chem.* **100**, 9703 (1996).
- ¹⁴H. G. Hertz, in *The Chemical Physics of Solvation, Part B Spectroscopy of Solvation*, edited by R. R. Dogonadze, E. Kálman, A. A. Kornyshev, and J. Ulstrup (Elsevier, Amsterdam, 1986), Chap. 7.
- ¹⁵K. Hashimoto and K. Morokuma, *Chem. Phys. Lett.* **223**, 423 (1994).
- ¹⁶T. Asada and K. Nishimoto, *Chem. Phys. Lett.* **232**, 518 (1995).
- ¹⁷L. M. Ramaniah, M. Bernasconi, and M. Parrinello, *J. Chem. Phys.* **109**, 6839 (1998).
- ¹⁸C. P. Petersen and M. S. Gordon, *J. Phys. Chem. A* **103**, 4162 (1999).
- ¹⁹G. Peslherbe, B. M. Ladanyi, and J. T. Hynes, *J. Phys. Chem. A* **104**, 4533 (2000).
- ²⁰L. X. Dang, J. E. Rice, J. Caldwell, and P. A. Kollman, *J. Am. Chem. Soc.* **113**, 2481 (1991).
- ²¹S.-B. Zhu and G. W. Robinson, *J. Chem. Phys.* **97**, 4336 (1992).
- ²²D. E. Smith and L. X. Dang, *J. Chem. Phys.* **100**, 3757 (1994).
- ²³K. Hermansson and M. Wójcik, *J. Phys. Chem.* **102**, 6089 (1998).
- ²⁴A. Chandra, *Phys. Rev. Lett.* **85**, 768 (2000).
- ²⁵R. Jimenez, G. R. Fleming, P. V. Kumar, and M. Maroncelli, *Nature (London)* **369**, 471 (1994).
- ²⁶H. Graener, G. Seifert, and A. Laubereau, *Phys. Rev. Lett.* **66**, 2092 (1991).
- ²⁷S. Woutersen, U. Emmerichs, and H. J. Bakker, *Science* **278**, 658 (1997).
- ²⁸R. Laenen, C. Rauscher, and A. Laubereau, *Phys. Rev. Lett.* **80**, 2622 (1998).
- ²⁹S. Woutersen, U. Emmerichs, H.-K. Nienhuys, and H. J. Bakker, *Phys. Rev. Lett.* **81**, 1106 (1998).
- ³⁰G. M. Gale, G. Gallot, F. Hache, N. Lascoux, S. Bratos, and J.-C. Leicknam, *Phys. Rev. Lett.* **82**, 1068 (1999).
- ³¹S. Woutersen and H. J. Bakker, *Phys. Rev. Lett.* **83**, 2077 (1999).
- ³²S. Woutersen and H. J. Bakker, *Nature (London)* **402**, 507 (1999).
- ³³J. Deak, S. Rhea, L. Iwaki, and D. Dlott, *J. Phys. Chem. A* **104**, 4866 (2000).
- ³⁴R. Laenen, T. Roth, and A. Laubereau, *Phys. Rev. Lett.* **85**, 50 (2000).
- ³⁵M. Kropman and H. J. Bakker, *Science* **291**, 2118 (2001).
- ³⁶R. E. Miller, *Science* **240**, 447 (1988).
- ³⁷H.-K. Nienhuys, S. Woutersen, R. A. van Santen, and H. J. Bakker, *J. Chem. Phys.* **111**, 1494 (1999).
- ³⁸A. Staib and J. T. Hynes, *Chem. Phys. Lett.* **204**, 197 (1993).
- ³⁹A. Nitzan and J. Jortner, *Mol. Phys.* **25**, 713 (1973).
- ⁴⁰A. Novak, *Struct. Bonding (Berlin)* **18**, 177 (1974).
- ⁴¹W. Mikenda, *J. Mol. Struct.* **147**, 1 (1986).
- ⁴²W. Mikenda and S. Steinböck, *J. Mol. Struct.* **384**, 159 (1996).
- ⁴³S. Mukamel, *Principles of Nonlinear Optical Spectroscopy* (Oxford University Press, New York, 1995).
- ⁴⁴M. J. Wójcik, J. Lindgren, and J. Tegenfeldt, *Chem. Phys. Lett.* **99**, 112 (1983).
- ⁴⁵G. N. Robertson and J. Yarwood, *Chem. Phys.* **32**, 267 (1978).
- ⁴⁶M. Bonn, M. J. P. Brugmans, A. W. Kleyn, R. A. van Santen, and H. J. Bakker, *Phys. Rev. Lett.* **76**, 2440 (1996).